Generation of mature T cells from human hematopoietic stem and progenitor cells in artificial thymic organoids

Christopher S Seet[1], Chongbin He[2], Michael T Bethune[3], Suwen Li[2], Brent Chick[2], Eric H Gschweng[4], Yuhua Zhu[2], Kenneth Kim[2], Donald B Kohn[4–7], David Baltimore[3], Gay M Crooks[2,5–8] & Amélie Montel-Hagen[2,8]

Studies of human T cell development require robust model systems that recapitulate the full span of thymopoiesis, from hematopoietic stem and progenitor cells (HSPCs) through to mature T cells. Existing *in vitro* models induce T cell commitment from human HSPCs; however, differentiation into mature CD3$^+$TCR-αβ$^+$ single-positive CD8$^+$ or CD4$^+$ cells is limited. We describe here a serum-free, artificial thymic organoid (ATO) system that supports efficient and reproducible *in vitro* differentiation and positive selection of conventional human T cells from all sources of HSPCs. ATO-derived T cells exhibited mature naive phenotypes, a diverse T cell receptor (TCR) repertoire and TCR-dependent function. ATOs initiated with TCR-engineered HSPCs produced T cells with antigen-specific cytotoxicity and near-complete lack of endogenous TCR Vβ expression, consistent with allelic exclusion of Vβ-encoding loci. ATOs provide a robust tool for studying human T cell differentiation and for the future development of stem-cell-based engineered T cell therapies.

Due to the spatiotemporal complexity of T cell development in the thymus, *in vitro* models of T cell differentiation have thus far been unable to fully recapitulate human T cell development. A major advance was the discovery that mouse stromal cell lines expressing a Notch ligand could support *in vitro* T cell differentiation from mouse or human HSPCs, as in the classic OP9-DL1 co-culture system[1–3]. In this and similar monolayer systems, human cord blood (CB) HSPCs undergo T lineage commitment and rapid early T cell differentiation to generate CD7$^+$ pro-T cells, followed by CD4 'immature single-positive' (ISP) precursors around day 20, and CD4$^+$CD8$^+$ double-positive (DP) precursors around day 30 (ref. 3). Despite this, positive selection of T cell precursors with productively rearranged TCRs is impaired in OP9-DL1 co-culture, and consequently few CD3$^+$CD8$^+$ or CD4$^+$ SP T cells develop[2–5]. By day 60–70 of co-culture on OP9-DL1, mature CD8 SP cells represent at most 2–4% of the total amount of cultured cells[5]. Improved maturation has been reported using CD34$^+$ HSPCs isolated from the human postnatal thymus[6] a population largely composed of lineage-committed pro-T cells[7]. However, T cell maturation on OP9-DL1 is particularly inefficient using mobilized peripheral blood (PB) and bone marrow (BM) HSPCs, the latter giving ~10% of the DP and CD3$^+$TCR-αβ$^+$ cell yields seen with CB cultures[8].

We and others have shown that three-dimensional (3D) organoid systems using mouse[9–11] or human[12] primary thymic stroma support improved positive selection and maturation of human T cells *in vitro*. However, these systems are difficult to use given their dependence on primary thymic tissue and their high experimental variability.

We report here the development of an ATO system based on a delta-like canonical Notch ligand 1 (*DLL1*)-expressing stromal cell line and serum-free, off-the-shelf components that support robust differentiation, positive selection and maturation of human CD3$^+$TCR-αβ$^+$ CD8 SP and CD4 SP T cells from CB, BM and PB CD34$^+$ HSPCs. Differentiation was efficient whether initiated with CD34$^+$CD3$^-$ HSPCs, hematopoietic stem cells (HSCs) or lymphoid progenitors. T cell differentiation in ATOs followed a phenotypic progression that closely recapitulated human thymopoiesis, and it was associated with long-term maintenance of CD34$^+$ T cell progenitors.

Both CD3$^+$ CD8 SP and CD3$^+$ CD4 SP mature T cells that developed in ATOs showed an antigen-naive phenotype, a diverse TCR repertoire, and cytokine production and proliferation in response to antigenic stimuli. ATOs also supported highly efficient differentiation of TCR-engineered, antigen-specific T cells from HSPCs that were transduced with constructs encoding MHC class I–restricted TCRs specific for the tumor-associated antigens NY-ESO-1 and MART-1. ATO-derived engineered T cells showed a naive phenotype, as well as *in vitro* and *in vivo* antigen-specific cytotoxicity. Moreover, these cells lacked endogenous TCR Vβ expression, consistent with induction of allelic exclusion by the transduced TCR-encoding construct during early T cell differentiation, suggesting a new approach for the generation of potentially

[1]Division of Hematology–Oncology, Department of Medicine, David Geffen School of Medicine (DGSOM), University of California Los Angeles (UCLA), Los Angeles, California, USA. [2]Department of Pathology and Laboratory Medicine, DGSOM, UCLA, Los Angeles, California, USA. [3]Division of Biology and Biological Engineering, California Institute of Technology (Caltech), Pasadena, California, USA. [4]Department of Microbiology, Immunology and Molecular Genetics, DGSOM, UCLA, Los Angeles, California, USA. [5]Division of Pediatric Hematology–Oncology, Department of Pediatrics, DGSOM, UCLA, Los Angeles, California, USA. [6]Eli and Edythe Broad Center of Regenerative Medicine and Stem Cell Research, UCLA, Los Angeles, California, USA. [7]Jonsson Comprehensive Cancer Center, UCLA, Los Angeles, California, USA. [8]These authors contributed equally to this work. Correspondence should be addressed to G.M.C. (gcrooks@mednet.ucla.edu).

RECEIVED 2 DECEMBER 2016; ACCEPTED 3 MARCH 2017; PUBLISHED ONLINE 3 APRIL 2017; DOI:10.1038/NMETH.4237

non-alloreactive engineered T cells for adoptive immunotherapy. Thus, ATOs are a standardized and highly efficient *in vitro* model of human T cell development that is readily amenable to genetic manipulation and may permit new approaches for the study of human T cell development.

RESULTS

An optimized artificial thymic organoid system

Our goal was to develop a robust system that supports *in vitro* differentiation and positive selection of human T cells from HSPCs from multiple sources. On the basis of studies using fetal thymic organ cultures (FTOCs) and reaggregated organoids, we hypothesized that 3D structure has a critical role in the positive selection of T cells. To avoid the use of primary thymic tissue, we tested *DLL1*-transduced stromal cell lines for their ability to support human T cell development. Because we and others have observed that the efficiency of T cell differentiation in the OP9-DL1 system is highly variable between different lots of fetal calf serum[13], we furthermore sought to identify serum-free conditions capable of supporting T cell differentiation in organoid cultures. To form organoids, we used a simple compaction reaggregation technique[9,12,14], in which stromal cells are aggregated with HSPCs by centrifugation and deployed on a cell culture insert at the air–fluid interface (**Fig. 1a**). Using this method, we identified a MS5 mouse BM stromal cell line[15] that had been transduced with human *DLL1* (hereafter referred to as MS5-hDLL1 cells) to be strongly supportive of human T cell differentiation and positive selection (as measured by the output of mature $CD3^+TCR\text{-}\alpha\beta^+$ CD8 SP cells) from T cell–depleted $CD34^+$ cord blood (CB) HSPCs. We also identified RPMI 1640 supplemented with B27, a multi-component additive used in neuronal and embryonic stem cell cultures[16], and Fms-related tyrosine kinase 3 (FLT3) ligand, interleukin (IL)-7 and ascorbic acid[17,18] (hereafter referred to as RB27) as a serum-free medium that supported robust human T cell differentiation in MS5-hDLL1 organoid cultures without lot-to-lot variation.

This optimized ATO system induced rapid and efficient T lineage commitment from CB $CD34^+CD3^-$ HSPCs, as shown by a predominance of $CD5^+CD7^+$ T lineage cells and the appearance of $CD4^+CD3^-$ ISP (CD4 ISP) and $CD4^+CD8^+$ (DP) T cell precursors by week 2 (**Fig. 1b**). More mature $CD3^+TCR\text{-}\alpha\beta^+$ cells emerged as early as week 4, and their number increased over time, accounting for ~30% of cells at week 6 (**Fig. 1b**). We also observed long-term maintenance of $CD34^+$ T cell progenitors in ATOs and were able to recapitulate the three phenotypic stages of thymic T cell progenitors: multipotent $CD34^+CD7^-CD1a^-$ early thymic progenitors (ETP) and developmentally downstream $CD34^+CD7+CD1a^-$ and $CD34^+CD7^+CD1a^+$ pro-T cells (**Fig. 1c**)[7,19]. Pro-T1 and pro-T2 progenitor phenotypes, based on an alternative classification scheme using CD5 and CD7 (ref. 20), were also readily identified within ATO $CD34^+$ cell population (**Fig. 1c**). Consistent with a T-lineage-biased ATO microenvironment, $CD19^+$ B cell frequency was low and decreased over time, and NK and myeloid frequencies remained low throughout (**Fig. 1b**,**d**). The frequency of $CD3^+TCR\text{-}\alpha\beta^+$ T cells in ATOs was highly consistent across experiments and included CD8 SP and, to a lesser extent, CD4 SP T cells, which was consistent with the occurrence of the phenomenon of positive selection in ATOs (**Fig. 1d**). A smaller population of $CD3^+TCR\text{-}\gamma\delta^+$ T cells was also consistently seen (**Fig. 1d**). Histological analyses of ATOs demonstrated the formation of dense tissue architecture with abundant lymphoid cells (**Supplementary Fig. 1**), clusters of which expressed CD3 (**Fig. 1e**).

Each ATO typically generated ~2×10^6 total cells at 6 weeks (**Fig. 1f**); however, cell yield per HSPC was inversely related to the number of HSPCs seeded and to the ratio of HSPCs to stromal cells (**Supplementary Fig. 2a**). Frequencies of precursor and mature T cells in ATOs were similar across initial HSPC numbers and ratios (**Supplementary Fig. 2b**), with the exception of ATOs that were generated with large numbers of stromal cells (6×10^5 per ATO), which showed impaired T cell maturation. Thus, smaller ATOs (typically 7,500 HSPCs and 1.5×10^5 stromal cells at a 1:20 ratio) were used for further experiments, and they showed high reproducibility of cell output and T cell differentiation across technical replicates ($n = 11$), independent of the lot of B27 used (**Supplementary Fig. 3a**–**d**). Of translational relevance, efficient T cell differentiation and cell output was also seen in ATOs that were cultured either with xeno-free B27 (**Supplementary Fig. 3e**,**f**) or using irradiated MS5-hDLL1 stromal cells (**Supplementary Fig. 3g**–**j**). Recovery of hematopoietic cells generated in ATOs after simple mechanical disruption and filtration resulted in >99% $CD45^+$ hematopoietic cells (**Supplementary Fig. 3k**).

Direct comparison of ATOs to the OP9-DL1 monolayer culture system revealed a similar efficiency of T lineage commitment (percentage $CD7^+CD5^+$ cells) but markedly superior generation of both DP and $CD3^+TCR\text{-}\alpha\beta^+$ T cells at 4 and 6 weeks (**Fig. 2a**–**d** and **Supplementary Fig. 4**). Improved positive selection was particularly evident in the prevalence of mature $CD3^+TCR\text{-}\alpha\beta^+$ CD8 SP T cells in ATOs but not in OP9-DL1 monolayers (**Fig. 2b**–**d** and **Supplementary Fig. 4**). Crossover experiments testing the effect of cell culture variables revealed that optimal positive selection and T cell maturation required all three components of the ATO system—3D structure, MS5-hDLL1 stromal cells and RB27 medium—as neither monolayer cultures using ATO components nor OP9-DL1 cells in 3D organoids supported T cell development (**Supplementary Fig. 5**). The parental MS5 cell line (which lacks *DLL1* expression) did not support T cell development in either monolayer or 3D cultures, consistent with a requirement for Notch signaling for T cell development (**Supplementary Fig. 5a**).

Thymopoiesis and naive T cell development in ATOs

We next compared T cell differentiation in ATOs to that in the postnatal human thymus. Week 12 CB ATOs showed a similar frequency of $CD34^+$ pro-T cells and T-lineage-committed ($CD5^+CD7^+$) cells to those in the thymus (**Fig. 3a**). Similarly to that seen in the thymus, most of the $CD3^+$ T cells in ATOs were $TCR\text{-}\alpha\beta^+$ (**Fig. 3a**). The frequencies of mature $CD3^+TCR\text{-}\alpha\beta^+$ CD8 SP and CD4 SP T cells in ATOs increased between weeks 6 and 12 (**Fig. 3b** and **Supplementary Fig. 6a**) and showed a reversed CD4:CD8 ratio as compared to that seen in the thymus.

Similarly to that observed in the thymus, ATO-derived $CD3^+TCR\text{-}\alpha\beta^+$ CD8 SP and $CD3^+TCR\text{-}\alpha\beta^+$ CD4 SP T cells transited from a DP-like 'immature naive' ($CD45RA^-CD45RO^+CD27^+CCR7^-CD1A^{hi}$) to a 'mature naive' ($CD45RA^+CD45RO^-CD27^+CCR7^+CD1a^{lo}$) phenotype[21,22] (**Fig. 3c** and **Supplementary Fig. 6a**–**c**). Both immature and mature naive T cell subsets co-expressed CD62L and CD28, with subset co-expression of CD127 and CD31, the latter of which is associated with recent

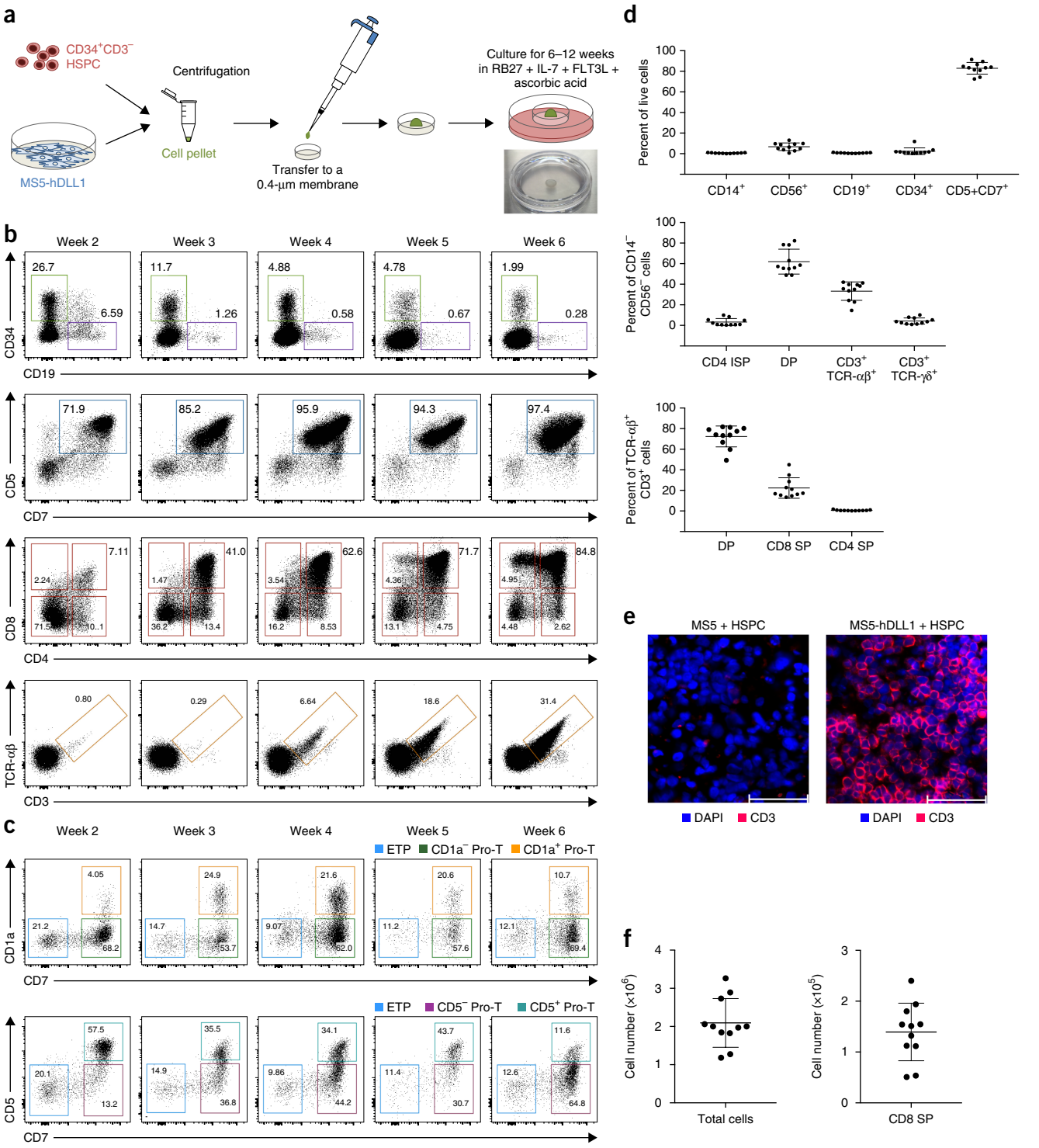

Figure 1 | Human T cell development in the ATO system. (**a**) Schematic of the ATO model. Image shows the appearance of a typical ATO attached to cell culture insert at 6 weeks (shown after removal from culture well). (**b**) Representative kinetic analysis ($n = 3$) of T cell differentiation from CB CD34$^+$CD3$^-$ HSPCs at the indicated time points, gated on CD14$^-$ and CD56$^-$ cells to exclude monocytes and NK cells, respectively. (**c**) Maintenance of early CD34$^+$ thymic T cell progenitor phenotypes in ATOs based on two classification schemes, both gated on CD34$^+$ cells as shown in **b** ($n = 3$). (**d**) Frequencies of cell types in ATOs ($n = 11$) at 6 weeks. Top, frequencies of monocytes (CD14$^+$), NK cells (CD56$^+$), B cells (CD19$^+$), HSPCs (CD34$^+$) and T lineage cell (CD7$^+$CD5$^+$) (gated on total live cells). Middle, T cell precursor and TCR$^+$ T cell frequencies (gated on CD14$^-$CD56$^-$ cells). Bottom, frequency of DP and mature CD8 and CD4 SP T cells (gated on CD3$^+$TCR-αβ$^+$ cells). (**e**) Representative immunofluorescence analysis ($n = 3$) for CD3 expression in week 4 organoids generated with CB HSPCs and MS-5 cells (left) or with MS5-hDLL1 cells (i.e., ATOs) (right). Nuclei were stained with DAPI. Scale bars, 50 μm. (**f**) Numbers of total live cells (left) and CD3$^+$TCR-αβ$^+$ CD8 SP T cells (right) generated per ATO at week 6 from 7.5×10^3 to 22.5×10^3 CB HSPCs per ATO. Data are shown for 11 independent experiments. In **d**,**f**, error bars indicate s.d.

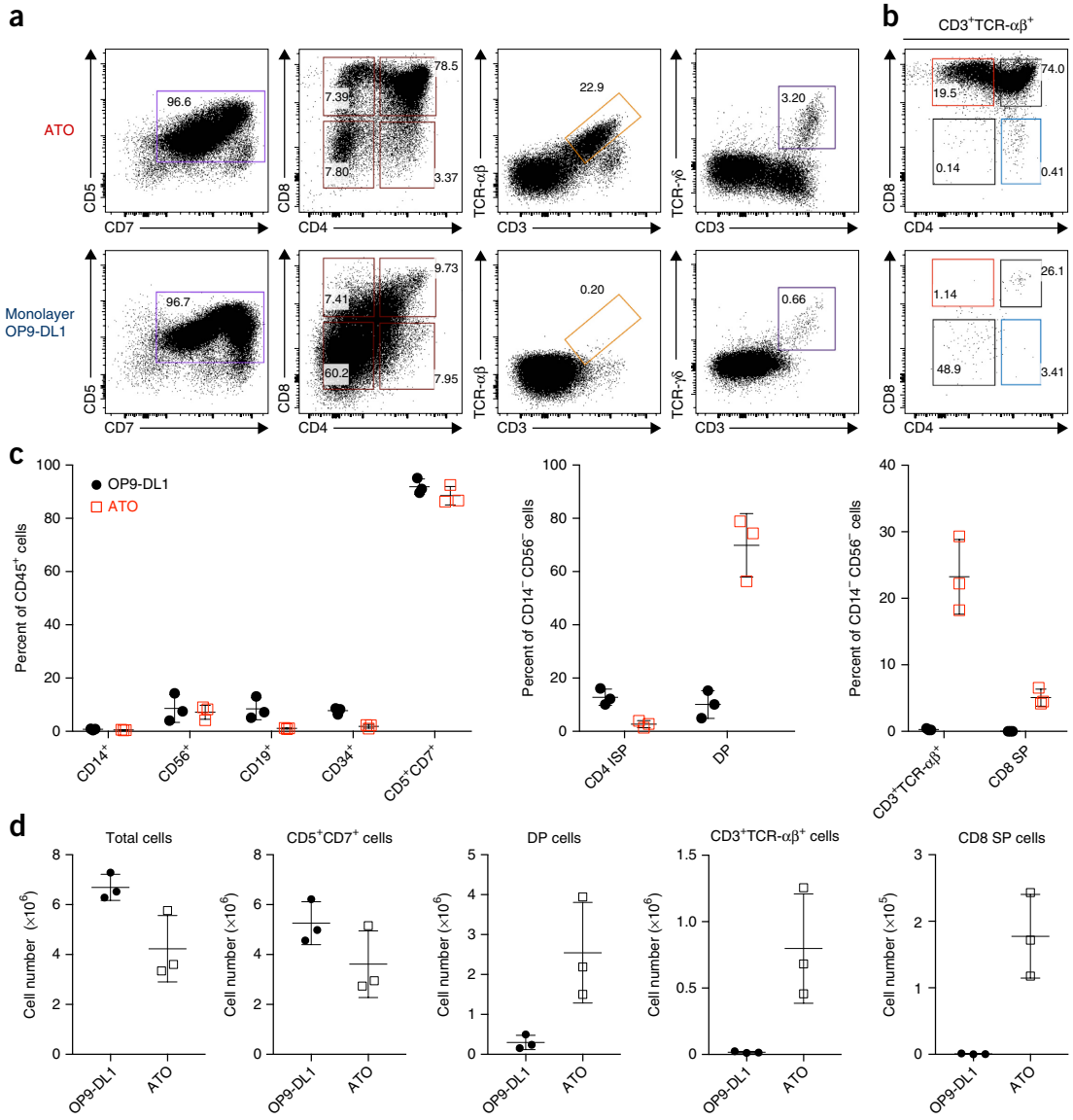

Figure 2 | Enhanced positive selection in the ATO system as compared to that in OP9-DL1 monolayers. CD34$^+$CD3$^-$ HSPCs from the same CB donor were used to initiate ATOs or standard OP9-DL1 monolayer cultures (containing 20% FBS) in parallel, followed by analysis using flow cytometry and cell counting. Shown are data from 6-week cultures. (**a**,**b**) Representative flow cytometry profiles (n = 3) of cells gated on total CD14$^-$CD56$^-$ cells (**a**) and CD3$^+$TCR-αβ$^+$ cells (**b**). (**c**,**d**) Frequencies of monocytes (CD14$^+$), NK cells (CD56$^+$), B cells (CD19$^+$), HSPCs (CD34$^+$) and T lineage cells (CD7$^+$CD5$^+$) (gated on total CD45$^+$ cells), CD4 ISP and DP T cell precursors, and CD3$^+$TCR-αβ$^+$ and CD3$^+$TCR-αβ$^+$ CD8 SP mature T cells (gated on CD14$^-$CD56$^-$ cells) in OP9-DL1 monolayer co-cultures versus those in ATOs at 6 weeks of culture (**c**) and absolute numbers of T cell subsets at week 6 in OP9-DL1 co-cultures versus ATOs using the frequency data shown in **c** (**d**). In **d**, OP9-DL1 cultures were each initiated with 1.5 × 10^4 CD34$^+$CD3$^-$ CB HSPCs cells, and ATOs were each initiated with 7.5 × 10^3 HSPCs from the same CB unit, with technical duplicate ATOs harvested and pooled at 6 weeks for comparison of cell counts. In **c**,**d**, bars represent the mean and s.d. of three independent experiments.

thymic emigrant T cells in the blood[23] (**Supplementary Fig. 6b**,**c**). The activation marker CD25 was not expressed on ATO-derived CD8 SP T cells, but it was observed on a subset of CD4 SP T cells (**Supplementary Fig. 6b**,**c**). Taken together, these data show remarkable fidelity of T cell differentiation in ATOs as compared to that in the human thymus, which culminates in the emergence of naive T cells that are phenotypically similar to those in the thymus and blood[24,25].

Given the absence of thymic epithelial cells, and the late emergence and relatively low frequencies of mature CD4 SP T cells, we postulated that MHC class II–mediated positive selection may rely on the development of rare dendritic cells in ATOs. Indeed, HLA-DR$^+$ cells were present in ATOs at low frequencies, and these included monocytes, B cells, and plasmacytoid, CLEC9A$^+$ and CD1c$^+$ dendritic cells (**Supplementary Fig. 6d**), all of which were also present in the thymus, in agreement with previous reports[26,27] (**Supplementary Fig. 6e**).

T cell differentiation from multiple HSPC sources and subsets

In addition to CB, we observed efficient T cell differentiation in ATOs from clinically relevant HSPC sources, i.e., adult BM, granulocyte-colony-stimulating factor (G-CSF)-mobilized PB (MPB) and nonmobilized PB (**Fig. 4a–d** and **Supplementary Fig. 7a**,**b**). Kinetics of T cell differentiation varied between cells

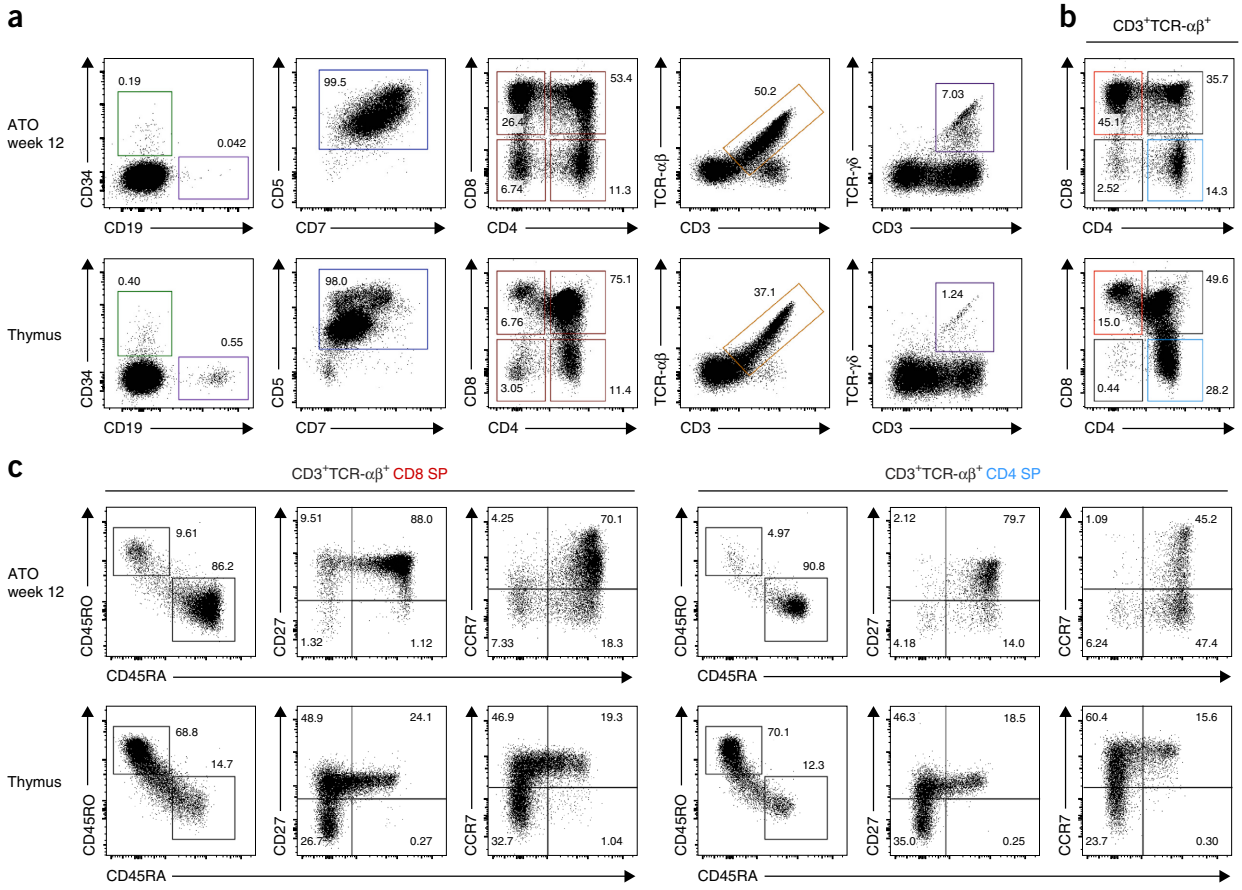

Figure 3 | Recapitulation of thymopoiesis and naive T cell development in ATOs. (**a**,**b**) Representative flow cytometry analysis comparing T cell differentiation in CB ATOs at 12 weeks (top) and human postnatal thymocytes (bottom), gated on total CD14$^-$CD56$^-$ (**a**) and on CD3$^+$TCR-αβ$^+$ (**b**) cells. (**c**) Generation of immature (CD45RA$^-$CD45RO$^+$) and mature (CD45RA$^+$CD45RO$^-$) naive T cells in ATOs or thymus (gated on CD3$^+$TCR-αβ$^+$ cells, with CD8 SP or CD4 SP subgates indicated). Throughout, data are representative of three independent experiments.

from different sources (**Fig. 4c**), with thymic CD34$^+$ cells predictably showing the fastest differentiation; however, T cell output was similar irrespective of the source (**Fig. 4d**). Enriched HSC fractions (Lin$^-$CD34$^+$CD38$^-$)[28] from CB, BM or MPB also demonstrated efficient T cell differentiation in ATOs (**Fig. 4e**,**f** and **Supplementary Fig. 7c**,**d**).

ATOs also supported T cell differentiation from highly purified lymphoid progenitors that were isolated from adult BM (**Fig. 4g**,**h**). Lymphoid-primed multipotent progenitors (LMPPs)[29] and CD24$^-$ common lymphoid progenitors[30] (CLPs) generated T cells to a greater extent than unfractionated CD34$^+$Lin$^-$ HSPCs (**Supplementary Fig. 7e**,**f**). In contrast, CD24$^+$ CLPs, which possess primarily B and NK cell potential[30,31], resulted in poor T cell output in ATOs (**Fig. 4g**,**h** and **Supplementary Fig. 7e**). Thus, ATOs can serve as a tool for evaluating T lineage potential in HSPC populations.

TCR diversity and function of ATO-derived T cells

Similarly to that observed in the thymus, *RAG1* and *RAG2* were expressed in DP T cells derived from ATOs, consistent with rearrangement of TCR-encoding genes (hereafter referred to as TCR genes) (**Supplementary Fig. 8a**). Flow cytometric analysis of ATO-derived CD3$^+$TCR-αβ$^+$ CD8 SP (**Fig. 5a**) and CD3$^+$TCR-αβ$^+$ CD4 SP (**Supplementary Fig. 8b**) T cells revealed notably similar usage of TCR Vβ families to those of corresponding naive T cells from human thymi. Physiological TCR diversity was confirmed by deep sequencing of the sequences encoding the TCR Vα and Vβ complementarity-determining region 3 (CDR3) regions in ATO-derived CD3$^+$TCR-αβ$^+$ CD8 SP T cells and their comparison to the sequences from both thymic and PB naive CD8 SP T cells (**Fig. 5b**,**c**). Notably, we did not observe skewed Vα or Vβ usage in ATO-derived T cells, which argued against the predominance of unconventional T cell lineages or clonally expanded T cells.

CD8 SP T cells isolated from ATOs demonstrated polyfunctional production of interferon (IFN)-γ, tumor necrosis factor (TNF)-α and IL-2 in response to treatment with phorbol 12-myristate 13-acetate (PMA) and ionomycin (**Fig. 5d**), showed upregulation of CD25 and 4-1BB, and proliferated in response to treatment with anti-CD3, anti-CD28 and IL-2 (**Fig. 5e**,**f**). CD4 SP cells that were freshly isolated from ATOs produced IFN-γ and IL-2 in response to PMA and ionomycin treatment, and they proliferated in response to treatment with anti-CD3, anti-CD28 and IL-2 (**Supplementary Fig. 8c–e**).

In vitro generation of naive TCR-engineered T cells in ATOs

We next explored whether ATOs could be used for the *in vitro* generation of naive TCR-engineered T cells. CB CD34$^+$CD3$^-$ HSPCs were transduced with a lentiviral vector encoding codon-optimized α and β chains of a HLA-A*02:01-restricted

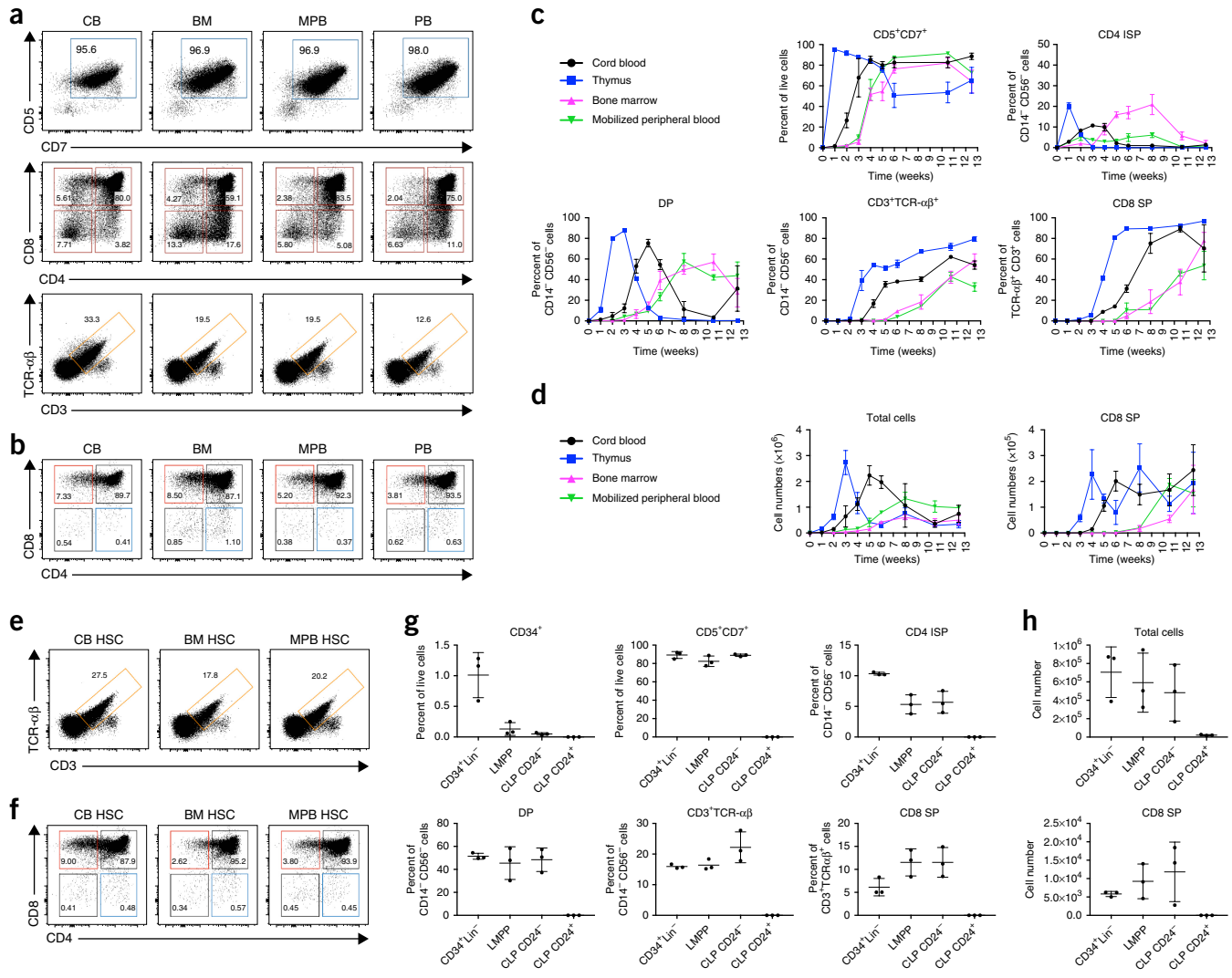

Figure 4 | Generation of T cells from multiple HSPC sources and subsets. (**a**,**b**) Representative analysis (n = 3) showing efficient T cell development in week 6 ATOs initiated with CD34$^+$CD3$^-$ HSPCs from human CB, adult BM, G-CSF-mobilized PB (MPB) or nonmobilized PB (PB). Cells were gated on total CD14$^-$CD56$^-$ cells (**a**) or on CD3$^+$TCR-αβ$^+$ T cells (**b**). (**c**) T cell differentiation kinetics over 12 weeks in ATOs generated from 7,500 CD34$^+$CD3$^-$ cells isolated from CB, neonatal thymi, BM or MPB. Mean and s.d. of T cell precursor and mature T cell frequencies are shown from three technical replicates per tissue. Data are representative of two different experiments. (**d**) Numbers of total cells and of CD3$^+$TCR-αβ$^+$ CD8 SP T cells from the ATO experiments shown in **c**. (**e**,**f**) T cell differentiation from HSC-enriched (Lin$^-$CD34$^+$CD38$^-$) fractions from CB, BM or MPB in week 6 ATOs, gated on CD14$^-$CD56$^-$ cells (**e**) and CD3$^+$TCR-αβ$^+$ T cells (**f**). Data are representative of independent experiments (CB, n = 3; BM, n = 2; MPB, n = 1). (**g**) T cell differentiation potential of adult BM total HSPCs (CD34$^+$Lin$^-$) and purified progenitor (LMPP and CLP) subsets in ATOs at week 6; frequencies of CD34$^+$ HSPCs, total T lineage cells (CD5$^+$CD7$^+$) and different T cell subsets are shown. (**h**) Numbers of total cells and CD3$^+$TCR-αβ$^+$ CD8 SP T cells from ATOs shown in **g**. In **g**,**h**, mean and s.d. of technical triplicates are shown, and data are representative of three independent experiments.

TCR specific for the NY-ESO-1$_{157–165}$ peptide[32] (hereafter referred to as TCR-transduced HSPCs). At 7 weeks of culture, ATOs derived from TCR-transduced cells showed a similar frequency of CD7$^+$CD5$^+$ T lineage cells as those from the mock-transduced controls but markedly increased CD3$^+$TCR-αβ$^+$ T cells, the majority of which expressed the exogenous TCR, as detected by a tetramer or an antibody specific for the exogenous Vβ13.1 chain (**Fig. 6a**). The frequency of CD3$^+$TCR-αβ$^+$ CD8 SP T cells that were generated from TCR-transduced HSPCs was similar to that of the CD3$^+$TCR-αβ$^+$ CD8 SP T cells from mock-transduced HPSCs; however, TCR transduction resulted in accelerated maturation from an immature (CD45RA$^-$CD45RO$^+$CD27$^-$CCR7$^-$CD1a^{hi}) to a mature (CD45RA$^+$CD45RO$^-$CD27$^+$CCR7$^+$CD1a^{lo}) naive T cell phenotype (**Fig. 6a**). Because antigen-specific T cells with an unconventional CD8-αα phenotype have been reported in the OP9-DL1 system[33], we confirmed that tetramer$^+$ T cells from ATOs displayed a conventional CD8-αβ phenotype and lacked expression of CD16 or CD56, markers associated with NK cells and innate-like T cells (**Fig. 6b**).

TCR transduction also significantly enhanced cell yield from ATOs (average ~500 cells per HSPC) (**Fig. 6c**), the majority of which were tetramer$^+$CD3$^+$ CD8 SP T cells. Thus, by 7 weeks of culture a single ATO that was initiated with 7,500 TCR-transduced HSPCs generated on average ~4 × 10^6 cells, of which approximately 15% (6 × 10^5) were mature naive tetramer$^+$CD3$^+$ CD8 SP CD45RA$^+$CD45RO$^-$ antigen-specific T cells (**Fig. 6a**,**c**).

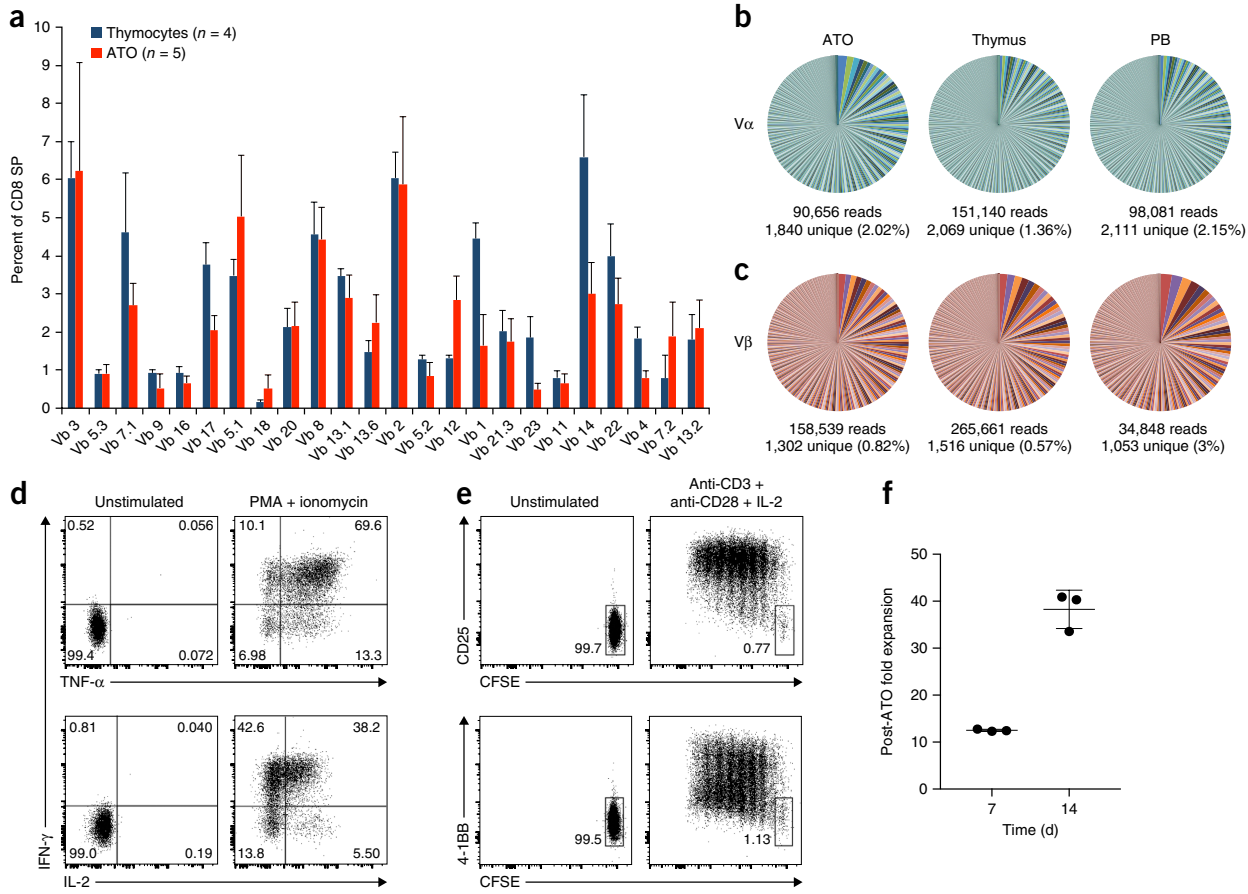

Figure 5 | TCR diversity and function of ATO-derived T cells. (**a**) Generation of TCR diversity in CD3⁺TCR-αβ⁺ CD8 SP T cells from week 7 ATOs ($n = 5$) or human thymi ($n = 4$), as shown by flow cytometric analysis of the frequency of TCR Vβ family expression. (**b**,**c**) TCR clonotype diversity in CD3⁺TCR-αβ⁺ CD8 SP T cells from ATOs and the thymus, and from naive T cells in the PB, by deep sequencing of the gene encoding the TCR Vα (**b**) or TCR Vβ (**c**) CDR3 regions. Frequency of individual clonotypes is shown. Data are representative of three independent experiments. (**d**) Polyfunctional cytokine production by ATO-derived CD3⁺TCR-αβ⁺ CD8 SP T cells after treatment with PMA + ionomycin for 6 h. Data are representative of three individual experiments. (**e**) Proliferation (as measured by dilution of CFSE, which is a fluorescent dye used to monitor cell division) and activation (upregulation of CD25 and 4-1BB) of ATO-derived CD3⁺TCR-αβ⁺ CD8 SP cells after 5 d of treatment with anti-CD3, anti-CD28 and IL-2. Data are representative of two individual experiments. (**f**) Post-ATO expansion of ATO-derived CD3⁺TCR-αβ⁺ CD8 SP T cells relative to the starting cell number in response to treatment with anti-CD3, anti-CD28 and IL-2 for 7 d or 14 d. The mean and s.d. of technical triplicates are shown, and data are representative of three independent experiments.

ATO-derived antigen-specific CD8 SP T cells showed polyfunctional cytokine production (IFN-γ, TNF-α and IL-2), degranulation (as assessed by CD107a membrane mobilization; **Fig. 6d**) and proliferation (**Fig. 6e**) in response to artificial antigen-presenting cells (aAPCs) expressing CD80 and a cognate HLA-A*02:01–NY-ESO-1 single-chain trimer but not to irrelevant HLA-A*02:01–MART-1-expressing aAPCs or to parental K562 cells. Furthermore, these T cells could be expanded by treatment with anti-CD3- and anti-CD28-coated beads and either IL-2 or IL-7 and IL-15 (**Fig. 6f**). A previous report of TCR-engineered T cells that were derived using the OP9-DL1 system reported loss of CD8-β expression following repeated *in vitro* stimulation[33]; although a subpopulation of ATO-derived tetramer⁺ CD8 SP T cells was CD8-β⁻ following re-stimulation with anti-CD3- and anti-CD28-coated beads, the majority of cells maintained a conventional CD8-αβ phenotype (**Supplementary Fig. 9a**).

Flow cytometric analysis of Vβ diversity in ATO-derived TCR-engineered T cells revealed that >98% of tetramer⁺CD3⁺ CD8 SP T cells expressed only the exogenous Vβ13.1 segment (**Fig. 6g** and **Supplementary Fig. 9b**), suggesting that allelic exclusion of both endogenous Vβ loci occurred during differentiation of TCR-engineered T cells in ATOs.

To test whether these findings could be extended beyond the NY-ESO-1-specific TCR, we generated ATOs using CB HSPCs that were transduced with a construct expressing a HLA-A*02:01-restricted TCR specific for MART-1 (ref. 34). Tetramer⁺CD3⁺ CD8 SP cells isolated from these ATOs demonstrated a naive T cell phenotype (**Supplementary Fig. 9c**), and they upregulated IFN-γ and mobilized CD107a in response to MART-1 but not NY-ESO-1 aAPCs (**Supplementary Fig. 9d**).

We next tested antigen-specific cytotoxicity of ATO-derived TCR-engineered T cells. Purified NY-ESO-1-specific CD8 SP T cells that were isolated from ATOs of TCR-transduced HSPCs and activated for 36 h potently induced apoptosis in cell lines expressing the cognate peptide–MHC complex (pMHC) (either K562 cells transduced with an HLA-A*02:01–NY-ESO-1 single-chain trimer (SCT) or the HLA-A*02:01–U266 multiple myeloma cell line, which endogenously expresses NY-ESO-1), but they showed little activity against parental K562 cells or K562 cells that expressed an irrelevant HLA-A*02:01–MART-1 SCT (**Fig. 6h** and

Supplementary Fig. 9e). Consistent with their naive state, prior activation of ATO-derived antigen-specific T cells was required for cytotoxicity. Loss of antigen specificity was not observed following prolonged (14 d) *in vitro* expansion, indicating retention of a conventional T cell phenotype (**Supplementary Fig. 9f**); furthermore, cytotoxicity was similar to that of TCR-transduced PB CD8$^+$ T cells that had been expanded for the same amount of time (**Supplementary Fig. 9f**). Consistent with these results,

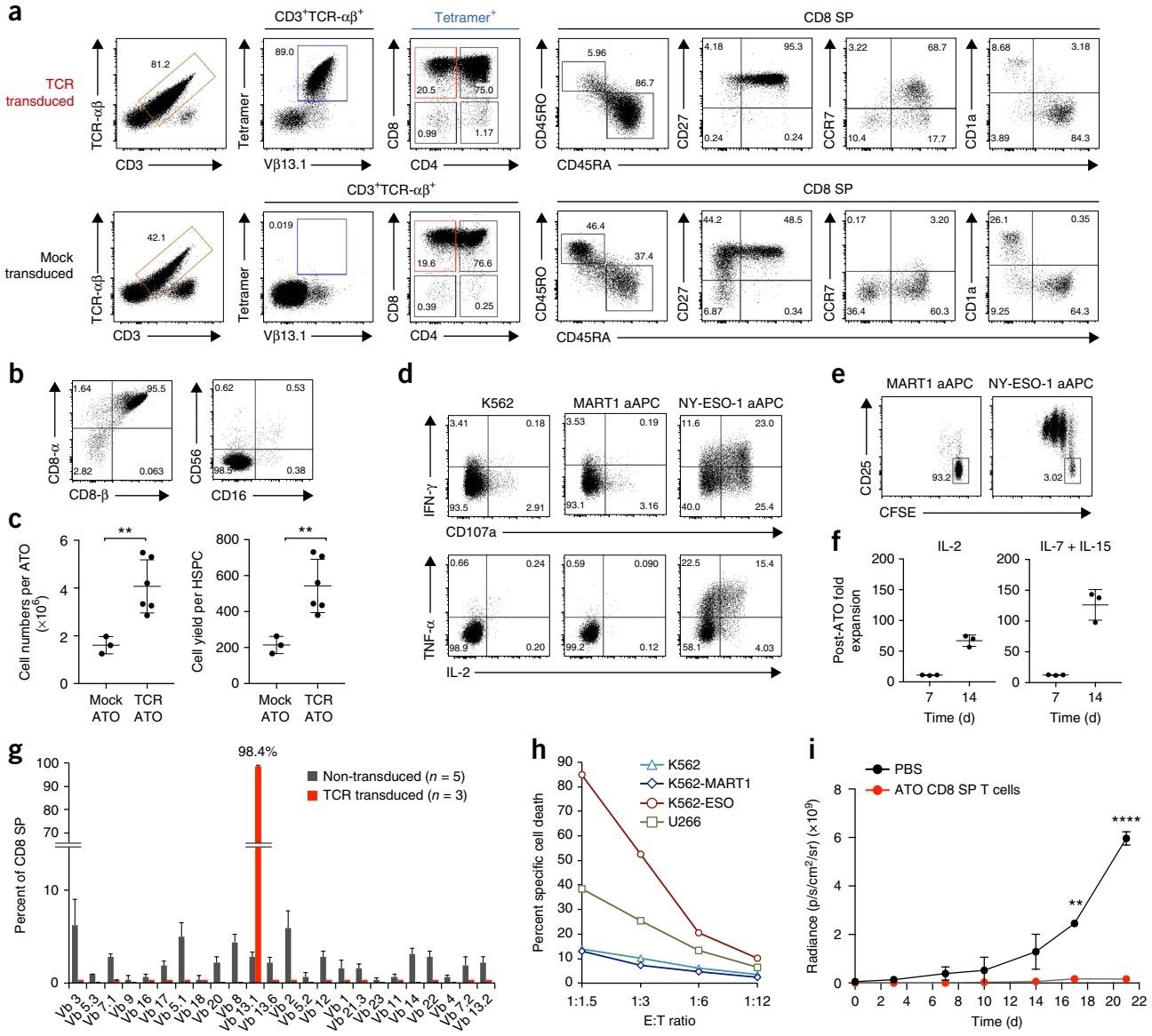

Figure 6 | Differentiation and allelic exclusion of TCR-engineered T cells in ATOs. (**a**) Representative analysis ($n = 3$) for the generation of HLA-A*0201–NY-ESO-$1_{157–165}$-specific TCR-engineered (or mock) T cells in week 7 ATOs that were initiated with CB HSPCs. Cells were gated on CD14$^-$CD56$^-$ cells. (**b**) Conventional T cell phenotype of CD3$^+$TCR-αβ$^+$tetramer$^+$ T cells from TCR-transduced CB ATOs. Data are representative of three independent experiments. (**c**) Cell output from ATOs generated with 7.5 × 10^3 to 18 × 10^3 starting CB HSPCs. Mean and s.d. of independent experiments are shown (mock, $n = 3$; TCR, $n = 8$). $^{**}P = 0.002$ by two-tailed unpaired *t*-test). (**d**) Cytokine production and CD107a membrane mobilization of tetramer$^+$CD3$^+$ CD8 SP T cells in response to K562 cells or to K562 aAPCs expressing an irrelevant (MART-1) or a cognate (NY-ESO-1) SCT. Data are representative of three independent experiments. (**e**) Proliferation (as measured by CFSE dilution) and activation (as measured by CD25 upregulation) of ATO-derived CD3$^+$tetramer$^+$ CD8 SP T cells in response to irrelevant (MART1) or cognate (NY-ESO-1) aAPCs for 72 h. Data are representative of two independent experiments. (**f**) Post-ATO expansion of CD3$^+$TCR-αβ$^+$ CD8 SP T cells (isolated from TCR-transduced ATOs) in response to anti-CD3, anti-CD28 and either IL-2 or IL-7 and IL-15 treatment. Mean and s.d. of technical triplicates are shown; data are representative of three independent experiments. (**g**) Allelic exclusion by flow cytometry of endogenous TCR Vβ in CD3$^+$TCR-αβ$^+$tetramer$^+$ CD8 SP cells isolated from ATOs of TCR-transduced cells ($n = 3$) versus those from nontransduced cells ($n = 5$). Error bars represent s.d. (**h**) *In vitro* cytotoxicity assay, in which CD8 SP T cells from HLA-A*02:01–NY-ESO-$1_{157–165}$-specific TCR-transduced ATOs were activated for 36 h and co-incubated with K562, K562 aAPCs (NY-ESO-1 or MART-1) or the HLA-A*02:01 U266 cell line which expresses NY-ESO-1 endogenously. Percentage cell death was determined by annexin V staining. Data are representative of two independent experiments. E:T, effector:target. (**i**) *In vivo* tumor control by ATO-derived TCR-engineered T cells. CD8 SP T cells from TCR-transduced ATOs were activated and expanded for 14 d. 4.5 × 10^6 tetramer$^+$ T cells or PBS was injected intravenously into NSG mice that had subcutaneously been implanted 3 d earlier with luciferase$^+$ K562-ESO tumor cells, and serial bioluminescence was recorded. Mean and s.d. for each group is shown (PBS, $n = 2$; TCR-transduced T cells, $n = 3$). $^{**}P = 0.00033$ and $^{****}P = 0.000066$ by two-tailed unpaired *t*-test.

ATO-derived TCR-engineered T cells were able to significantly control disease progression in immunodeficient NSG mice that had been subcutaneously engrafted with antigen-expressing K562 tumors (**Fig. 6i**).

DISCUSSION

We present here an *in vitro* system that efficiently initiates and sustains the normal stages of T cell commitment and differentiation from human HSPCs, culminating in the production of mature, naive $CD3^+TCR\text{-}\alpha\beta^+$ CD8 SP and $CD3^+TCR\text{-}\alpha\beta^+$ CD4 SP T cells that closely resemble naive T cells from the thymus and blood.

Enhanced positive selection of T cell in ATOs, relative to that in existing methods, was strictly dependent on both the 3D structure and the stromal cell line used, as monolayer cultures set up with ATO components resulted in inefficient T cell maturation, as did 3D organoid cultures using OP9-DL1 cells. We have, however, observed mature T cell development in ATOs using *DLL1*-transduced immortalized human BM stromal cells, and although efficiency is lower than that for MS5-hDLL1 cells, this indicates that neither species-specific nor MS5-specific factors underlie T cell positive selection in ATOs. We also predict that other Notch ligands, such as DLL4, should be effective in driving T cell development in ATOs.

A specific role for 3D structure in the positive selection of T cells is consistent with the reported ability of FTOCs and reaggregated primary thymic stromal organoids to permit T cell maturation, even though it occurs at low efficiency[10–12]. 3D interactions may support positive selection by increasing the valence and/or duration of contact between T cell precursors and the selective ligands (such as pMHC), facilitating cross-talk between stromal and hematopoietic cells or exerting developmental signals on T cell precursors through mechanical forces and/or metabolic gradients not otherwise possible in 2D cultures. The formation of thymic-like spatial niches that segregate developing T cells from stromal signals and/or Notch ligands during development may be another possible mechanism at work in ATOs. In the absence of thymic epithelial cells in ATOs, we hypothesize that selective MHC I ligands for the positive selection of CD8 SP cells are ubiquitously presented by hematopoietic cells within the ATOs, as has been suggested in the OP9-DL1 system[6] but that positive selection of CD4 SP cells occurs via MHC class II presentation by dendritic cells that develop within ATOs, with their rarity possibly underlying the bias toward $CD8^+$ T cell development in this system. The nature of these and other specific mechanisms of T cell selection can now be readily investigated using the ATO system in conjunction with model TCR–antigen systems.

Differentiation of TCR-engineered T cells from HPSCs has been reported using the OP9-DL1 system; however, as with non-transduced HSPCs, positive selection and generation of mature $CD3^+$ T cells is impaired (typically representing only 0–2% of the cells in the cultures), with the highest efficiencies being achieved using thymic $CD34^+$ cells[33,35,36]. In comparison, ATOs strongly supported the differentiation and positive selection of mature $CD3^+$ TCR-engineered T cells from CB HSPCs.

In contrast to TCR-transduced PB T cells, which require activation and prolonged expansion, *in vitro* generation of naive antigen-specific T cells may offer distinct therapeutic advantages for adoptive cell therapy based on studies correlating earlier T cell differentiation state with *in vivo* efficacy[24,37,38]. Nontransduced and TCR-transduced ATOs showed accumulation of naive $CD3^+$ CD8 SP T cells over time, with concomitant decrease in DPs, consistent with the absence of T cell egress. Despite this, mature T cells in ATOs retained a naive phenotype, absence of activation markers, and required activation–priming for effective cytotoxicity. TCR transduction of HSPCs also resulted in near-complete allelic exclusion of endogenous Vβ TCR loci, consistent with findings from *in vivo* studies of TCR-transduced mouse and human HSPCs[34,39,40]. The expression of potentially alloreactive endogenous TCRs on engineered PB T cells is a major barrier to the development of off-the-shelf adoptive T cell therapies, and current approaches to mitigate donor T cell alloreactivity, such as gene editing[41–43] or the use of virus-specific T cells[44], require extensive cell manipulation, which could potentially compromise function. We illustrate here that ATOs can be used to exploit developmental allelic exclusion of endogenous TCR expression as a novel strategy for generating potentially non-alloreactive antigen-specific T cells for immunotherapy. ATOs are thus a new tool for the study and development of stem-cell-based engineered T cell therapies, given the ease of genetically manipulating both hematopoietic and stromal compartments, and the ability to produce naive, unperturbed antigen-specific T cells.

Finally, the ATO system offers technical simplicity, reproducibility and potential scalability. The use of serum-free medium avoids the marked variability observed in monolayer systems[13], and the ability to maintain ATOs intact for the duration of culture (up to 20 weeks) with simple medium changes reduces labor through avoiding the frequent transfer of cells onto fresh stromal cells that are required by monolayer systems[2,3,13]. The simplicity of the ATO system permits straightforward adoption of the method in laboratories interested in studying human T cell development and engineered T cell therapies.

METHODS

Methods, including statements of data availability and any associated accession codes and references, are available in the online version of the paper.

Note: Any Supplementary Information and Source Data files are available in the online version of the paper.

ACKNOWLEDGMENTS

We thank J. Scholes and F. Codrea at the UCLA Broad Stem Cell Research Center (BSCRC) Flow Cytometry Core for assistance with FACS sorting, R. Chan for assistance with specimen processing, C. Parekh (Children's Hospital Los Angeles) for generous assistance with thymus samples, M. Sehl (UCLA) for assistance with MPB collection, and A. Cooper (UCLA) for helpful advice and discussion. We thank I. Antoshechkin (Millard and Muriel Jacobs Genetics and Genomics Laboratory, Caltech), who developed the method for, and who assisted with, TCR sequencing analysis, A. Ribas (UCLA) for the NY-ESO-1 and MART-1 TCR constructs, J. Zuniger-Pflucker (University of Toronto) for OP9-DL1 cells, L. Coulombel for MS-5 cells and J. Chute (UCLA) for U266 cells. This work was supported by the NIH (grants R01 AG049753 (G.M.C.), 1R21AI119927 (G.M.C. and A.M.-H.), P01 HL073104 (G.M.C. and D.B.K.) and T32HL066992 (C.S.S.)), the Tower Cancer Research Foundation (C.S.S.), a UCLA BSCRC Innovation award (G.M.C. and D.B.K.) and a BSCRC Clinical Fellowship (C.S.S.). M.T.B. and D.B. are supported by Prostate Cancer Foundation Challenge Award 15CHAL02, and M.T.B. is the recipient of a Jane Coffin Childs Postdoctoral Fellowship. Core services were supported by the UCLA Jonsson Comprehensive Cancer Center shared facility (TPCL, grant 5P30CA016042), the UCLA Immunogenetics Center, the UCLA Center for AIDS Research Virology Core Lab and the UCLA AIDS Institute (grant 5P30 AI028697), and the Millard and Muriel Jacobs Genetics and Genomics Laboratory at Caltech.

AUTHOR CONTRIBUTIONS

C.S.S. and A.M.-H. designed and performed experiments, analyzed data, prepared figures and co-wrote the manuscript; C.H. performed histological experiments

and, with B.C., assisted with *in vivo* experiments; S.L. assisted with ATO analysis and T cell functional assays; K.K. assisted with ATO cultures; Y.Z. performed human specimen processing and cultured the cell lines; E.H.G. and D.B.K. provided critical reagents and conceptual advice and edited the manuscript; M.T.B. and D.B. devised the approach for, and performed, TCR repertoire sequencing analysis and provided critical reagents; and G.M.C. and A.M.-H. co-directed the project and co-wrote the manuscript.

COMPETING FINANCIAL INTERESTS

The authors declare competing financial interests: details are available in the online version of the paper.

1. Schmitt, T.M. & Zúñiga-Pflücker, J.C. Induction of T cell development from hematopoietic progenitor cells by delta-like-1 *in vitro*. *Immunity* **17**, 749–756 (2002).
2. De Smedt, M., Hoebeke, I. & Plum, J. Human bone marrow CD34$^+$ progenitor cells mature to T cells on OP9-DL1 stromal cell line without thymus microenvironment. *Blood Cells Mol. Dis.* **33**, 227–232 (2004).
3. La Motte-Mohs, R.N., Herer, E. & Zúñiga-Pflücker, J.C. Induction of T cell development from human cord blood hematopoietic stem cells by Delta-like 1 *in vitro*. *Blood* **105**, 1431–1439 (2005).
4. de Pooter, R. & Zúñiga-Pflücker, J.C. T cell potential and development *in vitro*: the OP9-DL1 approach. *Curr. Opin. Immunol.* **19**, 163–168 (2007).
5. Awong, G., Herer, E., La Motte-Mohs, R.N. & Zúñiga-Pflücker, J.C. Human CD8 T cells generated *in vitro* from hematopoietic stem cells are functionally mature. *BMC Immunol.* **12**, 22 (2011).
6. Van Coppernolle, S. *et al.* Functionally mature CD4 and CD8 TCR-αβ cells are generated in OP9-DL1 cultures from human CD34$^+$ hematopoietic cells. *J. Immunol.* **183**, 4859–4870 (2009).
7. Hao, Q.L. *et al.* Human intrathymic lineage commitment is marked by differential CD7 expression: identification of CD7$^-$ lympho-myeloid thymic progenitors. *Blood* **111**, 1318–1326 (2008).
8. De Smedt, M. *et al.* T lymphoid differentiation potential measured *in vitro* is higher in CD34$^+$CD38$^{-/lo}$ hematopoietic stem cells from umbilical cord blood than from bone marrow and is an intrinsic property of the cells. *Haematologica* **96**, 646–654 (2011).
9. Anderson, G., Jenkinson, E.J., Moore, N.C. & Owen, J.J.T. MHC class II–positive epithelium and mesenchyme cells are both required for T cell development in the thymus. *Nature* **362**, 70–73 (1993).
10. Plum, J., De Smedt, M., Defresne, M.P., Leclercq, G. & Vandekerckhove, B. Human CD34$^+$ fetal liver stem cells differentiate to T cells in a mouse thymic microenvironment. *Blood* **84**, 1587–1593 (1994).
11. Poznansky, M.C. *et al.* Efficient generation of human T cells from a tissue-engineered thymic organoid. *Nat. Biotechnol.* **18**, 729–734 (2000).
12. Chung, B. *et al.* Engineering the human thymic microenvironment to support thymopoiesis *in vivo*. *Stem Cells* **32**, 2386–2396 (2014).
13. Awong, G., Motte-Mohs, R.N.L. & Zúñiga-Pflücker, J.C. *In vitro* human T cell development directed by notch–ligand interactions. in *Hematopoietic Stem Cell Protocols.* (ed. Bunting, K.D.) 135–142 (Humana Press, 2008).
14. Sheridan, J.M., Taoudi, S., Medvinsky, A. & Blackburn, C.C. A novel method for the generation of reaggregated organotypic cultures that permits juxtaposition of defined cell populations. *Genesis* **47**, 346–351 (2009).
15. Itoh, K. *et al.* Reproducible establishment of hemopoietic supportive stromal cell lines from murine bone marrow. *Exp. Hematol.* **17**, 145–153 (1989).
16. Brewer, G.J., Torricelli, J.R., Evege, E.K. & Price, P.J. Optimized survival of hippocampal neurons in B27-supplemented Neurobasal, a new serum-free medium combination. *J. Neurosci. Res.* **35**, 567–576 (1993).
17. Huijskens, M.J.A.J. *et al.* Technical advance: ascorbic acid induces development of double-positive T cells from human hematopoietic stem cells in the absence of stromal cells. *J. Leukoc. Biol.* **96**, 1165–1175 (2014).
18. Manning, J. *et al.* Vitamin C promotes maturation of T cells. *Antioxid. Redox Signal.* **19**, 2054–2067 (2013).
19. Casero, D. *et al.* Long noncoding RNA profiling of human lymphoid progenitor cells reveals transcriptional divergence of B cell and T cell lineages. *Nat. Immunol.* **16**, 1282–1291 (2015).
20. Awong, G. *et al.* Characterization *in vitro* and engraftment potential *in vivo* of human progenitor T cells generated from hematopoietic stem cells. *Blood* **114**, 972–982 (2009).
21. Vanhecke, D., Leclercq, G., Plum, J. & Vandekerckhove, B. Characterization of distinct stages during the differentiation of human CD69$^+$CD3$^+$ thymocytes and identification of thymic emigrants. *J. Immunol.* **155**, 1862–1872 (1995).
22. Res, P., Blom, B., Hori, T., Weijer, K. & Spits, H. Downregulation of CD1 marks acquisition of functional maturation of human thymocytes and defines a control point in late stages of human T cell development. *J. Exp. Med.* **185**, 141–151 (1997).
23. Kimmig, S. *et al.* Two subsets of naive T helper cells with distinct T cell receptor excision circle content in human adult peripheral blood. *J. Exp. Med.* **195**, 789–794 (2002).
24. Hinrichs, C.S. *et al.* Adoptively transferred effector cells derived from naive rather than central memory CD8$^+$ T cells mediate superior antitumor immunity. *Proc. Natl. Acad. Sci. USA* **106**, 17469–17474 (2009).
25. Restifo, N.P., Dudley, M.E. & Rosenberg, S.A. Adoptive immunotherapy or cancer: harnessing the T cell response. *Nat. Rev. Immunol.* **12**, 269–281 (2012).
26. Gurka, S., Dirks, S., Photiadis, J. & Kroczek, R.A. Expression analysis of surface molecules on human thymic dendritic cells with the 10th HLDA Workshop antibody panel. *Clin. Transl. Immunology* **4**, e47 (2015).
27. Martínez, V.G. *et al.* A discrete population of IFN-λ-expressing BDCA3^{hi} dendritic cells is present in human thymus. *Immunol. Cell Biol.* **93**, 673–678 (2015).
28. Hao, Q.L., Shah, A.J., Thiemann, F.T., Smogorzewska, E.M. & Crooks, G.M. A functional comparison of CD34$^+$CD38$^-$ cells in cord blood and bone marrow. *Blood* **86**, 3745–3753 (1995).
29. Kohn, L.A. *et al.* Lymphoid priming in human bone marrow begins before expression of CD10 with upregulation of L-selectin. *Nat. Immunol.* **13**, 963–971 (2012).
30. Six, E.M. *et al.* A human postnatal lymphoid progenitor capable of circulating and seeding the thymus. *J. Exp. Med.* **204**, 3085–3093 (2007).
31. Galy, A., Travis, M., Cen, D. & Chen, B. Human T, B, natural killer and dendritic cells arise from a common bone marrow progenitor cell subset. *Immunity* **3**, 459–473 (1995).
32. Gschweng, E.H. *et al.* HSV-sr39TK positron emission tomography and suicide gene elimination of human hematopoietic stem cells and their progeny in humanized mice. *Cancer Res.* **74**, 5173–5183 (2014).
33. Snauwaert, S. *et al. In vitro* generation of mature, naive antigen-specific CD8$^+$ T cells with a single T cell receptor by agonist selection. *Leukemia* **28**, 830–841 (2014).
34. Giannoni, F. *et al.* Allelic exclusion and peripheral reconstitution by TCR transgenic T cells arising from transduced human hematopoietic stem and progenitor cells. *Mol. Ther.* **21**, 1044–1054 (2013).
35. Zhao, Y. *et al.* Extrathymic generation of tumor-specific T cells from genetically engineered human hematopoietic stem cells via Notch signaling. *Cancer Res.* **67**, 2425–2429 (2007).
36. van Lent, A.U. *et al.* Functional human antigen-specific T cells produced *in vitro* using retroviral T cell receptor transfer into hematopoietic progenitors. *J. Immunol.* **179**, 4959–4968 (2007).
37. Gattinoni, L. *et al.* Acquisition of full effector function *in vitro* paradoxically impairs the *in vivo* antitumor efficacy of adoptively transferred CD8$^+$ T cells. *J. Clin. Invest.* **115**, 1616–1626 (2005).
38. Hinrichs, C.S. & Rosenberg, S.A. Exploiting the curative potential of adoptive T cell therapy for cancer. *Immunol. Rev.* **257**, 56–71 (2014).
39. Vatakis, D.N. *et al.* Introduction of exogenous T cell receptors into human hematopoietic progenitors results in exclusion of endogenous T cell receptor expression. *Mol. Ther.* **21**, 1055–1063 (2013).
40. Stärck, L., Popp, K., Pircher, H. & Uckert, W. Immunotherapy with TCR-redirected T cells: comparison of TCR-transduced and TCR-engineered hematopoietic stem cell–derived T cells. *J. Immunol.* **192**, 206–213 (2014).
41. Torikai, H. *et al.* A foundation for universal T cell–based immunotherapy: T cells engineered to express a CD19-specific chimeric antigen receptor and eliminate expression of endogenous TCR. *Blood* **119**, 5697–5705 (2012).
42. Berdien, B., Mock, U., Atanackovic, D. & Fehse, B. TALEN-mediated editing of endogenous T cell receptors facilitates efficient reprogramming of T lymphocytes by lentiviral gene transfer. *Gene Ther.* **21**, 539–548 (2014).
43. Poirot, L. *et al.* Multiplex genome-edited T cell manufacturing platform for 'off-the-shelf' adoptive T cell immunotherapies. *Cancer Res.* **75**, 3853–3864 (2015).
44. Themeli, M., Rivière, I. & Sadelain, M. New cell sources for T cell engineering and adoptive immunotherapy. *Cell Stem Cell* **16**, 357–366 (2015).

ONLINE METHODS

A protocol to aid users accompanies this article and is available as **Supplementary Protocol**; it has also been deposited in the Protocol Exchange[45].

Isolation of human CD34$^+$CD3$^-$ HSPCs. Neonatal umbilical CB was obtained from discarded cord and placental units from deliveries at UCLA. BM was obtained from healthy adult donors (ages 18–51) through discarded material from allogeneic BM donor harvests at UCLA or was purchased from AllCells Inc. (Alameda, CA). G-CSF-mobilized PB was obtained from consenting healthy adult donors (ages 44–60) who were undergoing apheresis for allogeneic stem cell transplant donation at UCLA. Nonmobilized PB was obtained from healthy adult donors through the UCLA CFAR Virology Core. All tissue samples were obtained under UCLA Institutional Review Board (IRB)-approved protocols or exemptions. All samples were enriched for mononuclear cells by Ficoll-Paque (GE Healthcare Life Sciences, Pittsburgh, PA) gradient centrifugation followed by positive selection of CD34$^+$ cells by magnetic cell sorting (MACS) using the CD34 MicroBead Kit UltraPure (Miltenyi Biotec, Auburn, CA). CD34$^+$-cell-enriched fractions were cryopreserved after MACS, unless otherwise noted. Prior to use, cells were thawed, and the residual T cells were depleted by FACS by sorting for CD34$^+$CD3$^-$ cells, which were immediately seeded into ATOs or transduced as described below. In some experiments, HSCs were enriched by FACS for Lin$^-$CD34$^+$CD38$^-$ cells before seeding in ATOs. HSPCs used in TCR transduction experiments were from HLA-A*02:01 + CB units. High-resolution HLA-A2 typing was performed by the UCLA Immunogenetics Center using sequence-specific oligonucleotide (SSO) beads.

Isolation of human bone marrow progenitor subsets. CD34$^+$ HSPCs were enriched from fresh BM aspirates, as described above, and immediately sorted by FACS for stem and progenitor populations based on positive expression of CD45 and the absence of expression of lineage markers (CD3, CD14, CD19, CD56 and CD235a; referred to as 'Lin$^-$') combined with the following markers: total HSPCs (CD34$^+$), HSC (CD34$^+$CD38$^-$CD45RA$^-$)[28,46], LMPP (CD34$^+$CD38$^+$CD45RA$^+$CD10$^-$CD62L^{hi})[29], CD24$^-$ CLP (CD34$^+$CD38$^+$CD45RA$^+$CD10$^+$CD24$^-$)[30] and CD24$^+$ CLP (CD34$^+$CD38$^+$CD45RA$^+$CD10$^+$ CD24$^+$)[30,31].

Isolation of human thymocytes. Postnatal human thymi were obtained under an IRB exemption as discarded waste from patients undergoing cardiac surgery at Children's Hospital Los Angeles (CHLA). Thymic fragments were finely dissected in RPMI medium (Cellgro) and disrupted by pipetting to release thymocytes into suspension, followed by passage through a 70-μm nylon strainer. Cells were analyzed fresh on the same or the following day. Flow cytometry analysis of thymic and ATO-derived T cell progenitors used the following surface phenotypes: early thymic progenitor (ETP; CD34$^+$CD7$^-$CD1a$^-$), CD1a$^-$ pro-T (CD34$^+$CD7$^+$CD1a$^-$) and CD1a$^+$ pro-T (CD34$^+$CD7$^+$CD1a$^+$) cells[7], or CD5$^-$ pro-T (pro-T1; CD34$^+$CD7$^+$CD5$^-$) and CD5$^+$ pro-T (pro-T2; CD34$^+$CD7$^+$CD5$^+$) cells[20]. Thymic and ATO-derived T cells and precursors were defined as CD14$^-$CD56$^-$ in combination with the following phenotypes: total T lineage cells (CD7$^+$CD5$^+$), double negative (DN; CD4$^-$CD8$^-$), CD4 ISP (CD5$^+$CD4$^+$CD3$^-$), double positive (DP; CD4$^+$CD8$^+$), CD8 SP (CD3$^+$TCR-αβ$^+$CD8$^+$CD4$^-$), CD4 SP (CD3$^+$TCR-αβ$^+$CD8$^-$CD4$^+$), immature naive (CD45RA$^-$CD45RO$^+$ that were CD8 SP or CD4 SP) and mature naive (CD45RA$^+$CD45RO$^-$ that were CD8 SP or CD4 SP). Immature and mature naive phenotypes were confirmed by co-staining for CD1a, CD27, CD28 and CCR7.

Isolation of primary human T cells. Thymic T cells were isolated from thymocyte preparations as described above, and PB and CB CD8$^+$ T cells were isolated from mononuclear cell fractions as described above. CD8$^+$ T cell isolation from all sources was by magnetic bead enrichment for CD8 SP T cells using the CD8$^+$ T cell Isolation Kit (Miltenyi Biotec). In some experiments, thymic T cells were further purified by FACS to deplete CD4 ISP or DP precursors, and PB T cells were further purified by FACS to isolate naive T cells (CD45RO$^-$CCR7$^+$).

Cell lines. The MS5 mouse stromal cell line[15] was obtained as a gift from Laure Coulombel and is commercially available from Leibniz Institute DSMZ–German Collection of Microorganisms and Cell Cultures, Braunschweig Germany (DSMZ no. ACC 441). To generate MS5-hDLL1 cells, we transduced MS5 cells with a lentiviral vector encoding human DLL1 and enhanced green fluorescent protein (eGFP). The top 5% of the cells with the highest expression of GFP were sorted by FACS and passaged in Dulbecco's modified Eagle's medium (DMEM; Cellgro) + 10% FCS (Gemini). Stable expression was confirmed by flow cytometry for GFP expression after several weeks of culture, and *DLL1* expression was confirmed by qRT–PCR and DNA sequencing; absence of mycoplasma contamination was confirmed. The OP9-DL1 cell line[1] (expressing mouse *Dll1*) was a gift from Dr. Juan Carlos Zúñiga-Pflücker (University of Toronto) and was passaged in MEMα (ThermoFisher Scientific, Grand Island, NY) + 20% FBS in 0.1% gelatin–coated flasks. The K562 cell line was obtained from the ATCC and maintained in RPMI + 10% FCS. K562 aAPCs were generated by co-transduction of K562 cells with lentiviral vectors encoding full-length human CD80 and HLA-A*02:01–β2M–NY-ESO-$1_{157–165}$ or HLA-A*02:01–β2M–MART-$1_{26–35}$ SCTs (provided by D.B.). K562 target cells were created by transduction of constructs encoding either of the SCTs without CD80. Luciferase–K562 target cells were created by sequential transduction of K562 cells with a firefly-luciferase-expressing lentiviral vector (provided by D.B.K.) followed by either of the SCT vectors. K562 transductants were FACS-sorted before use. The U266 multiple myeloma cell line was a gift from Dr. John Chute (UCLA) and maintained in RPMI + 10% FCS.

Artificial thymic organoid (ATO) cultures. MS5-hDLL1 (or MS5 or OP9-DL1, as noted) cells were harvested by trypsinization and resuspended in serum-free ATO culture medium ('RB27'), which was composed of RPMI 1640 (Corning, Manassas, VA), 4% B27 supplement (ThermoFisher Scientific, Grand Island, NY), 30 μM l-ascorbic acid 2-phosphate sesquimagnesium salt hydrate (Sigma-Aldrich, St. Louis, MO) reconstituted in PBS, 1% penicillin–streptomycin (Gemini Bio-Products, West Sacramento, CA), 1% Glutamax (ThermoFisher Scientific, Grand Island, NY), 5 ng/ml recombinant human FLT3 ligand (rhFLT3L) and 5 ng/ml recombinant human IL-7 (rhIL-7) (Peprotech, Rocky Hill, NJ). RB27 was made fresh weekly. 4% XenoFree B27 was

substituted for B27 in the indicated experiments. Depending on the experiment, 1.5×10^5 to 6×10^5 MS5-hDLL1 cells were combined with 3×10^2 to 1×10^5 purified $CD34^+CD3^-$ cells (or other HSPC populations, as indicated) per ATO in 1.5-ml microcentrifuge tubes and centrifuged at 300*g* for 5 min at 4 °C in a swinging-bucket centrifuge. Supernatants were carefully removed, and the cell pellet was resuspended by brief vortexing. For each ATO, a 0.4-μm Millicell Transwell insert (EMD Millipore, Billerica, MA; Cat. PICM0RG50) was placed in a 6-well plate containing 1 ml RB27 per well. To plate ATOs, inserts were taken out and rested on the edge of the plate to drain the excess medium. The cell slurry was adjusted to 5 μl per ATO, drawn up in with a 20-μl pipet tip and plated by forming a drop at the end of the pipet tip that was then gently deposited onto the cell insert. The cell insert was placed back in the well containing 1 ml RB27. Medium was changed completely every 3–4 d by aspiration from around the cell insert followed by replacement with 1 ml fresh RB27 + cytokines. ATOs were cultured in this fashion for up to 20 weeks. At the indicated times, ATO cells were harvested by adding FACS buffer (0.5% BSA and 2 mM EDTA in PBS) to each well and briefly disaggregating the ATO by pipetting with a 1 ml 'P1000' pipet tip, followed by passage through a 50-μm nylon strainer. In some experiments, single-cell suspensions of MS5-hDLL1 cells were γ-irradiated at the indicated doses before use in ATOs.

T cell monolayer co-cultures. OP9-DL1 monolayer cultures were set up as previously described[1,3,13]. Briefly, OP9-DL1 cells were seeded into 0.1% gelatin–coated 12-well plates 1–2 d before use to achieve 70–80% confluence. Medium was aspirated from monolayers, and 1.5×10^4 FACS-purified $CD34^+CD3^-$ HSPCs were plated on stromal monolayers in 2 ml of medium composed of MEMα, 20% FBS, 30 μM l-ascorbic acid, 5 ng/ml rhFLT3L and 5 ng/ml rhIL-7. In some experiments, MS5 or MS5-hDLL1 cells were substituted for OP9-DL1 cells, and RB27 was substituted as the culture medium. Cells were transferred to new stromal cell monolayers every 4–5 d by harvesting cells, filtering them through a 50-μm nylon strainer and re-plating them in fresh medium. When the cells reached confluence, they were split into multiple wells containing fresh stromal layers.

Lentiviral vectors and transduction. The full-length coding sequence of human *DLL1* was cloned by RT–PCR from a human universal reference RNA set (Agilent Technologies, Santa Clara, CA) into the third-generation lentiviral vector pCCL-c-MNDU3-X-IRES-eGFP[34] (provided by D.B.K.). Human *CD80* was similarly cloned into pCCL-c-MNDU3. The third-generation lentiviral vector encoding the codon-optimized α and β (Vb13.1) chains of a TCR specific for HLA-A*02:01–NY-ESO-$1_{157\text{-}165}$ (derived from the 1G4 TCR clone[47]) has previously been described[32] and was a gift from Dr. Antoni Ribas (UCLA). The codon-optimized HLA-A*02:01–MART-$1_{26\text{-}35}$-specific TCR (derived from the F5 TCR clone[48]) was provided by D.B.K. Coding sequences for HLA-A*02:01–β2-M–NY-ESO-$1_{157–165}$ and HLA-A*02:01–β2-M–MART-$1_{26–35}$ SCTs were provided by D.B. and subcloned into the pCCL-c-MNDU3-X-IRES-mStrawberry lentiviral vector. Packaging and concentration of lentivirus particles was performed as previously described[32]. Briefly, 293T cells (ATCC) were co-transfected with a lentiviral vector plasmid, pCMV-R8.9, and pCAGGS-VSVG using TransIT 293T (Mirus Bio, Madison, WI) for 17 h followed by treatment with 20 mM sodium butyrate for 8 h, followed by generation of cell supernatants in serum-free UltraCulture for 48 h. Supernatants were concentrated by tangential flow filtration using Amicon Ultra-15 100K filters (EMD Millipore, Billerica, MA) at 4,000*g* for 40 min at 4 °C and stored as aliquots at −80 °C. For HSPC transduction, 1×10^5 to 1×10^6 FACS-sorted $CD34^+CD3^-$ HSPCs were plated in 6-well nontreated plates coated with 20 μg/ml Retronectin (Clontech, Mountain View, CA) in 1 ml X-VIVO-15 (Lonza, Basel, Switzerland) supplemented with 50 ng/ml of recombinant human stem cell factor (SCF), FLT3L and thyropoietin (TPO), and 10 ng/ml IL-3 (Peprotech, Rocky Hill, NJ) for 12–18 h, after which the lentiviral supernatant was concentrated to a final concentration of 1×10^7 to 2×10^7 TU/ml. Mock-transduced cells were cultured in identical conditions without the addition of vector. Cells were harvested 24 h after transduction, washed and seeded into ATOs. For transduction of PB T cells, $CD8^+$ T cells from healthy donors were isolated by magnetic negative selection using the $CD8^+$ T cell Isolation Kit (Miltenyi Biotec) and activated and expanded in AIM V medium with 5% human AB serum with anti-CD3- and anti-CD28-coated beads (ThermoFisher Scientific) and 20 ng/ml IL-2 for 4 d before transduction, as previously described[32]. Transduced T cells were subsequently expanded in the presence of IL-2 (20 ng/ml) before use.

Immunohistochemistry. For hematoxylin and eosin (H&E)-stained images, ATOs were embedded in Histogel (ThermoFisher Scientific, Grand Island, NY) and fixed overnight in 10% neutral-buffered formalin (ThermoFisher Scientific, Grand Island, NY). 5-μm sections and H&E staining were performed by the UCLA Translational Pathology Core Laboratory (TPCL). For immunofluorescence imaging, ATOs were isolated by cutting the culture insert around each ATO with a scalpel, followed by embedding the membrane and ATO in Tissue-Tek OCT (VWR Radnor, PA) and freezing on dry ice. 5-μm frozen sections were fixed in 10% neutral-buffered formalin and stained with anti-CD3 (clone UCHT1; BioLegend, San Diego, CA) at a 1:50 dilution overnight at 4 °C followed by incubation with AlexaFluor-594-conjugated anti-mouse IgG (H+L) (Jackson ImmunoResearch, West Grove, PA) at room temperature. H&E-stained and immunofluorescence images were acquired on a Zeiss AzioImager M2 with AxioCam MRM and AxioVision software (Zeiss, Jena, Germany).

T cell cytokine assays. Mature CD8 SP or CD4 SP cells from ATOs were isolated by magnetic negative selection using the $CD8^+$ or $CD4^+$ Isolation Kits (Miltenyi Biotec) and sorted by FACS to further deplete $CD45RO^+$ cells (containing immature naive T cells and CD4 ISP precursors). Purified T cell populations were plated in 96-well U-bottom plates in 200 μl AIM V medium (ThermoFisher Scientific, Grand Island, NY) with 5% human AB serum (Gemini Bio-Products, West Sacramento, CA). PMA + ionomycin + protein transport inhibitor cocktail or a control protein transport inhibitor cocktail (eBioscience, San Diego, CA) was added to each well and incubated for 6 h. Cells were stained for CD3, CD4 and CD8 (BioLegend, San Diego, CA), as well as UV455 fixable viability dye (eBioscience, San Diego, CA), before fixation and permeabilization with an intracellular staining buffer kit (eBioscience, San Diego, CA) and intracellular staining

doi:10.1038/nmeth.4237

with antibodies against IFN-γ, TNF-α, IL-2, IL-4 or IL-17A (BioLegend, San Diego, CA).

T cell activation and proliferation assays. For CFSE proliferation assays, ATO-derived CD8 SP or CD4 SP T cells were isolated by negative selection MACS as described in the T cell cytokine assays subsection (with further FACS purification of CD4 SP T cells as described above) and labeled with 5 μM CFSE (BioLegend, San Diego, CA). Labeled cells were incubated with anti-CD3- and anti-CD28-coated beads (ThermoFisher Scientific, Grand Island, NY) in AIM V medium with 5% human AB serum and 20 ng/ml rhIL-2 (Peprotech, Rocky Hill, NJ), co-stained for CD25 or 4-1BB (BioLegend, San Diego, CA), and analyzed by flow cytometry on day 5. In some experiments, CFSE was substituted for CellTrace Violet (CTV; ThermoFisher) with labeling done as per the manufacturer's protocol. For *in vitro* cell expansion assays, 5×10^3 to 1×10^4 ATO-derived CD8 SP or CD4 SP T cells, isolated as described above, were plated in 96-well U-bottom plates in 200 μl and activated (or expanded) with anti-CD3- and anti-CD28-coated beads and either 20 ng/ml IL-2 or 5 ng/ml IL-7 and 5 ng/ml IL-15 (Peprotech). Beads were removed on day 4, and fresh medium and cytokines were added every 2–3 d, with re-plating into larger wells as needed. Cells were counted weekly with a hemacytometer. In some experiments, cells were re-stimulated with fresh anti-CD3- and anti-CD28-coated beads on day 14.

Artificial APC (aAPC) cytotoxic T lymphocyte (CTL) priming assay. 1×10^5 total ATO-derived CD8 SP T cells were isolated from week 6 TCR-transduced ATOs by MACS, as described above, and co-cultured with K562-derived aAPCs expressing CD80 and single-chain trimers of either HLA-A*02:01–B2M–NY-ESO-$1_{157–165}$ or HLA-A*02:01–B2M–MART-$1_{26–35}$ or with parental K562 cells in 96-well U-bottom plates in 200 μl AIM V with 5% human AB serum at a 2:1 T cell:aAPC ratio for 6 h. Allophycocyanin (APC)-conjugated CD107a-specific antibody (BioLegend, San Diego, CA) was added to wells at a 1:50 final dilution together with a protein transport inhibitor cocktail (eBioscience, San Diego, CA) for the duration of culture. Cells were then stained for surface markers, fixed, permeabilized and intracellularly stained for cytokines as described above.

TCR Vβ phenotypic analysis. Total cells from pooled week 7 ATOs or postnatal thymi were stained for CD3, CD4, CD8 and TCR-γδ, in conjunction with the IOTest Beta Mark TCR V Kit (Beckman Coulter, Indianapolis, IN). $CD3^+TCR\text{-}\gamma\delta^-CD8^+CD4^-$ cells were gated for analysis, and Vβ family usage was determined by percentage of $FITC^+$, PE^+ or $FITC^+PE^+$ cells, which represented three different Vβ-specific antibodies per tube. For Vβ analysis of TCR-transduced ATOs, total cells from week 6–7 ATOs were additionally labeled with an APC-conjugated HLA-A*02:01–NY-ESO-$1_{157–165}$ tetramer (MBL International, Woburn, MA) for 10 min before surface antibody staining, and cells were gated on a $CD3^+TCR\gamma\delta^-tetramer^+CD8^+CD4^-$ phenotype for Vβ analysis.

TCR repertoire sequencing. Total RNA was purified from 40,000–200,000 FACS-sorted ATO or thymic $CD3^+TCR\text{-}\alpha\beta^+$ CD8 SP or PB $CD3^+TCR\text{-}\alpha\beta^+CD8^+CD45RO^-CCR7^+$ naive $CD8^+$ T cells using the RNeasy Micro kit (Qiagen) according to the manufacturer's instructions. RNA concentration and quality were determined using the Agilent RNA 6000 Nano chip. A targeted cDNA library comprising rearranged genes encoding the TCR variable regions was prepared by 5′ random amplification of cDNA ends (RACE) using the SMARTer PCR cDNA Synthesis kit (Clontech) with modifications as follows. First-strand cDNA was prepared from 3.5–500.0 ng total RNA using the manufacturer's protocol but substituting a poly-dT primer (5′-T30VN-3′). Double-stranded TCR-α-encoding and TCR-β-encoding cDNA libraries were prepared separately by semi-nested PCR using the Advantage 2 PCR kit (Clontech). Initial amplification of cDNAs encoding TCR-α used 0.5 μl of the first-strand reaction (2.5 μl of 1:5 dilution in TE) with the manufacturer's forward Universal Primer Mix and a pair of reverse primers that bound *TRAC* (5′-GCCACAGCACTGTTGCTCTTGAAGTCC-3′). Semi-nested amplification of TCR-α-encoding cDNA was conducted with the manufacturer's forward Primer IIA and barcoded reverse primers that bound *TRAC* (5′- X5GGCAGGGTCAGGGTTCTGGAT-3′, where X5 is a 5-nt sample-specific barcode that enables sample pooling before deep-sequencing). Amplification of TCR-β-encoding cDNA was similar, but initial amplification was performed with a reverse primer that bound *TRBC* (5′- CCACCAGCTCAGCTCCACGTG-3′), and semi-nested amplification was conducted with barcoded primers that bound *TRBC* (5′- X5GGGAACACSTTKTTCAGGTCCTC-3′). TCR-α and TCR-β cDNA preparations were cleaned up using the DNA Clean and Concentrator-5 kit (Zymo Research). TCR-α and TCR-β cDNA preparations from up to ten samples were pooled before Illumina adaptor ligation and 2 × 150-bp paired-end sequencing on the MiSeq sequencer (Illumina). TCR rearrangements were identified by aligning reads that included the CDR3-encoding sequence to a custom reference sequence library comprising sequences encoding all human T cell receptor alpha variable (TRAV), T cell receptor alpha joining (TRAJ), T cell receptor beta variable (TRBV), T cell receptor beta diversity (TRBD) and T cell receptor beta joining (TRBJ) molecules contained in the International Immunogenetics Information System (IMGT) database[49]. After de-multiplexing using sample-specific barcodes, reads were aligned to a custom reference database comprising all possible combinations of human TRAV-, TRAJ-, TRBV-, TRBD- and TRBJ-encoding sequences downloaded from the IMGT database[49] using BLAT[50]. The best BLAT hits were identified with the pslCDnaFilter utility of the BLAT suite using '-maxAligns = 1 –ignoreIntrons' options, and clonotype frequencies were calculated using custom Perl scripts (available upon request).

***In vitro* cytotoxicity assays.** CD8 SP T cells were isolated from pooled ATOs, as described above, and were activated in 96-well round-bottom plated in AIM V medium with 5% human AB serum, anti-CD3- and anti-CD28-coated beads (ThermoFisher Scientific) and 20 ng/ml IL-2 for 36 h. For extended expansions, cells were cultured in IL-2 for up to 14 d. For cytotoxicity assays, twofold serial dilutions of T cells were plated in 96-well round-bottom plates starting at 1×10^5 cells per well in AIM V medium with 5% human AB serum. K562 target cells that were transduced with constructs expressing HLA-A*02:01–NY-ESO-$1_{157–165}$ or HLA-A*02:01–MART-$1_{26–35}$ single-chain trimers, or U266 multiple myeloma cells, were plated at 5×10^4 cells per well. Apoptotic cell death of target cells was quantified by annexin V and DAPI staining at 9 h. The percentage of antigen-specific T cells was

determined by tetramer staining at the start of assays and used to retrospectively calculate the effector:target (E:T) ratio of each well. T cell–specific cell death was calculated by subtracting the percentage of annexin V^+ target cells in wells that did not receive T cells from wells that received T cells.

***In vivo* tumor assays.** All animal experiments were conducted under a protocol approved by the UCLA Chancellor's Animal Research Committee. 4- to 6-week-old male NOD.Cg-Prkdcscid Il2rgtm1Wjl/SzJ (NSG) mice (Jackson Laboratory, Bar Harbor, Maine) were subcutaneously implanted with 2×10^5 K562 target cells that had been transduced with a construct encoding HLA-A*02:01–NY-ESO-$1_{157–165}$ single-chain trimer and firefly luciferase (as described above). Mice were imaged for tumor bioluminescence on day 3 by intraperitoneal injection of luciferin. ATO-derived CD8 SP T cells were isolated and activated and expanded, as described above, for 14 d. 5.7×10^6 T cells (containing 4.5×10^6 antigen-specific T cells, as determined by tetramer staining on the day of injection) were injected via retro-orbital vein on day 3 after tumor implantation. Injection of PBS into control mice was also performed. Tumor bioluminescence was repeated every 3–4 d for at least 21 d, after which the mice were euthanized based on disease burden criteria.

Flow cytometry and antibodies. All flow cytometry stains were performed in 0.5% BSA and 2 mM EDTA in PBS for 30 min on ice. FcX (BioLegend, San Diego, CA) was added to all samples for 5 min before antibody staining. For tetramer co-staining, PE- or APC-conjugated HLA-A*02:01–NY-ESO-$1_{157–165}$ or HLA-A*02:01–MART-$1_{26–35}$ tetramers (MBL International, Woburn, MA) were added to cells at a 1:50 final dilution at room temperature for 10 min before addition of antibodies for an additional 20 min on ice. DAPI was added to all samples before analysis. Analysis was performed on an LSRII Fortessa, and FACS was performed on an ARIA or ARIA-H instrument (BD Biosciences, San Jose, CA) at the UCLA Broad Stem Cell Research Center Flow Cytometry Core. For all analyses $DAPI^+$ cells were gated out, and single cells were gated based on forward scatter (FSC)-height (FSC-H) versus FSC-width (FSC-W) and side scatter (SSC)-H versus SSC-W. Monoclonal antibodies (specific clones in parentheses) used for surface and intracellular staining of the following molecules were obtained from BioLegend (San Diego, CA): CD1a (HI149), CD3 (UCHT1), CD4 (RPA-T4), CD5 (UCHT2), CD8 (SK1), CD10 (6H6), CD14 (M5E2), CD19 (HIB19), CD24 (ML5), CD25 (BC96), CD27 (O323), CD28 (CD28.2), CD31 (WM59), CD34 (581), CD38 (HIT2), CD45 (HI30), CD45RA (HI100), CD45RO (UCHL1), CD56 (HCD56), CD107a (H4A3), CD127 (A019D5), CD235a (HI264), CCR7 (G043H7), HLA-A2 (BB7.2), IFN-γ (4S.B3), IL-2 (MQ1-17H12), IL-4 (MP4-25D2), IL-17A (BL168), TCR-αβ (IP26), TCR-γδ (B1), TNF-α (Mab11), Vβ13.1 (H131) and human lineage cocktail (CD3, CD14, CD19, CD20, CD56). Antibodies to CD7 (M-T701) and CD62L (DREG-56) were obtained from BD Biosciences (San Jose, CA).

Statistical analysis. For **Figure 6c,i**, statistics were analyzed using a two-tailed unpaired *t*-test. Exact *n* values for all experiments are specified in the figure legends.

Data availability. The data that support the findings of this study are available from the corresponding author upon request. Sequences for the TCR-encoding genes from this study are available in the NCBI Gene Expression Omnibus repository under accession number GSE94968.

45. Seet, C.S., Crooks, G.M. & Montel-Hagen, A. Artificial thymic organoid cultures: *in vitro* human T cell differentiation from hematopoietic stem and progenitor cells. *Protoc. Exch.* (http://dx.doi.org/10.1038/protex.2017.062).
46. Majeti, R., Park, C.Y. & Weissman, I.L. Identification of a hierarchy of multipotent hematopoietic progenitors in human cord blood. *Cell Stem Cell* **1**, 635–645 (2007).
47. Robbins, P.F. *et al.* Single and dual amino acid substitutions in TCR CDRs can enhance antigen-specific T cell functions. *J. Immunol.* **180**, 6116–6131 (2008).
48. Johnson, L.A. *et al.* Gene transfer of tumor-reactive TCR confers both high avidity and tumor reactivity to nonreactive peripheral blood mononuclear cells and tumor-infiltrating lymphocytes. *J. Immunol.* **177**, 6548–6559 (2006).
49. Giudicelli, V., Chaume, D. & Lefranc, M.-P. IMGT/GENE-DB: a comprehensive database for human and mouse immunoglobulin and T cell receptor genes. *Nucleic Acids Res.* **33**, D256–D261 (2005).
50. Kent, W.J. BLAT—the BLAST-like alignment tool. *Genome Res.* **12**, 656–664 (2002).

doi:10.1038/nmeth.4237